Research Article

Naresh Mallireddy* and K. Siva

Investigation of Microstructural, Mechanical and Corrosion Properties of AA7010-TiB_2 in-situ Metal Matrix Composite

https://doi.org/10.1515/secm-2020-0010
Received Nov 27, 2019; accepted Mar 07, 2020

Abstract: Aluminum alloys with ceramic reinforced particulates are made prospective in aerospace, transportation, and industrial applications ampler to their low mass density, stiffness, and high specific strength. In this work, Aluminium Alloy(AA) 7010 - TiB_2 (Titanium Diboride) composites with different amounts of reinforcement (5, 7.5 and 10 wt.%) were produced by the exothermic reaction of halide salts K_2TiF_6 and KBF_4 added in 120% excess to the stoichiometric ratio with molten AA7010.The effect and dispersion of TiB_2 particulates in AA7010 were analyzed by microstructural, mechanical and corrosion behavior. The dispersion of reinforcement in the matrix alloy was analyzed by optical microscope and field emission scanning electron microscope (FESEM) images. X-ray diffraction patterns of the prepared composites reveal the formation of TiB_2 particles in the matrix alloy. Indeed samples are tested according to ASTM G34 standard for exfoliation corrosion rate by weight loss method. The result shows improved hardness, tensile strength and yield strength of composites to about 35%, 260%, and 240% respectively. The mechanical and corrosion resistance of 10% TiB_2 shows better results compared with matrix alloy and other concentrations of reinforcements.

Keywords: AA7010, TiB_2, Stir-casting method, exfoliation corrosion test

***Corresponding Author: Naresh Mallireddy:** Department of Automobile Engineering, Hindusthan College of Engineering and Technology, Coimbatore, Tamilnadu, 641032, India; Email: naresh.mallireddy@gmail.com; Tel.: +91-9626032235
K. Siva: Department of Mechanical Engineering, Hindusthan College of Engineering and Technology, Coimbatore, Tamilnadu, 641032, India

1 Introduction

Aluminium-ceramic reinforced metal matrix composites have been produced widely owing to their high strength-to-weight ratio, improved stiffness, better corrosion resistance, reduced density, and survival at high temperature, superior dampness and excellent dimensional stability [1–3]. These composites synthesized by ex-situ methods might lead to thermodynamic instability; segregation and poor adhesion of the reinforcements at the matrix interface [4, 5]. To overcome these limitations often induced in ex-situ synthesized composites in-situ methods are been prominent in recent years. Metal Matrix Composites synthesized by these techniques afford exceptional matrix-reinforcement bonding at the interface, uniform distribution of finer particles, stability of reinforcements thermodynamically and economical processing methods. An extensive range of ceramic reinforcements, like Al_2O_3, TiB_2, TiC, and SiC have been used to fabricate in-situ Aluminium Metal Matrix Composites [6]. Among these ceramic reinforcements, TiB_2 remains dominant in providing advanced phase strengthening for aluminium alloy as it holds a desirable physical and mechanical properties, comprising of better elastic modulus (560 GPa), high hardness (3400 HV), high melting point (3225°C) and excellent resistance to wear. In addition to that at the interface unfavorable intermetallic phases are not allowed by the TiB_2 reinforcement in the aluminium matrix alloy [7–9]. H.B.Michael Rajan *et al.* produced AA7075/TiB_2 (0, 3, 6 and 9 wt.%) in-situ composites through stir casting process and examined microhardness, Ultimate Tensile Strength (UTS), % elongation and microstructure. They discussed about the effect of reinforcement weight percentage on mechanical properties. The improvement of micro hardness and UTS were achieved due to good bonding and uniform dispersion of reinforcement at the interface. Fractography images reveal the presence of TiB_2 particles, which act as grain refinement leading to the formation of smaller voids in the developed composites [10]. J.Jeben Moses *et al.* developed an empirical relationship to predict the effects of various stir casting parameters such as stirring speed (S), casting temperature(T), stirrer blade angle(A), and stirring time(t) on AA6061/ 15% TiC aluminium metal matrix composite. They inferred that each parameter has an influence on the UTS of the composite due to the segregation and cluster formation of TiC particles at the interface [11]. Akshay Mohan Pujar and Chetan Kulakarni synthesized AA7175-TiB_2 composite by incorporating two salts of K_2TiF_6 and KBF_4 reacted exothermically with liquid aluminium alloy and they investigated the effect of reinforcement with different(5,7.5, and 10) wt.% of TiB_2 for mechanical and wear properties [12]. Fie Chen *et al.* fabricated Al-TiB_2 insitu composites with varying wt.% of 1, 4 and 7 by mechanical stirring at salt/ aluminium interface with optimized process parameters such as stirring start time, time of duration, and intensity of the stirring. It is observed that formation of severe agglomeration is suppressed by proper stirring intensity and duration. Yield strength (YS) and Ultimate Tensile Strength (UTS) of Al-7% TiB_2 are found to be 260% and 180% more than the base alloy. Fractography studies reveal that the composite follow ductile fracture in spite of stiff reinforcements [13]. As aircraft is becoming larger high strength to weight ratio materials like 2XXX and 7XXX alloys are needed, but these materials were found to be susceptible to stress corrosion cracking (SCC) and Exfoliation Corrosion (EXCO) [14, 15]. Ankur Chowdary *et al.* evaluated the Exfoliation Corrosion rate on aluminium alloy 7010 under T6 and T7 conditions. In their study the samples of AA7010 were subjected to forced condition environment created by making test solution containing extremely corrosive chemicals. The rate of exfoliation corrosion is been determined as per ASTMG34 standard. Samples are also tested for variation of electrical conductivity in the test solution before and after corrosion. The eddy current instrument is used to measure electrical conductivity. The corrosion rate and electrical conductivity of the aluminum alloy was found to be increased with increase upon heat treatment [16]. AA7010 is found to be having broad application in making aircraft and automobile structures due to their light weight and outstanding mechanical properties as well it was considered as significant pioneering material in aluminum alloys as it, substituted traditional AA 7075 in large die forging application [17, 18].

Understand the need of novel material for aerospace structural components with high strength to weight ratio. In current investigation, a new and light TiB_2 reinforced aluminum metal matrix composite has been synthesized by in-situ stir casting process. Along with, an effort is made to study the influence of TiB_2 for various wt.% on the microstructure, mechanical and corrosion properties of the developed composites.

Table 1: The chemical composition of AA7010

Alloy	Zn	Mg	Cu	Fe	Zr	Al
	wt.%					
AA7010	6.2	2.3	1.75	0.15	0.13	90.6

2 Materials and Methods

2.1 Material Selection

AA7010 (Al–Zn–Mg–Cu-Zr) is used as matrix alloy and the chemical composition is as shown in Table 1. In- organic salts namely, potassium tetrafluroborate (KBF_4) and potassium hexaflurotitanate (K_2TiF_6) have been used to synthesize the TiB_2 reinforcement by exothermic reaction of two salts with molten alloy. AA7010 and the two halide salts (98% purity) were procured from FENFE Metallurgicals, India and Sisco Research Laboratories Pvt. Ltd. (SRL), India respectively.

2.2 In-situ stir casting synthesis

Aluminium alloy 7010 reinforced with different concentrations of TiB_2 (5, 7.5 and 10 wt.%) were synthesized by in-situ stir casting process. The reinforcement was formed through the reaction of two halide salts namely potassium hexaflurotitanate (K_2TiF_6) and potassium tetrafluroborate (KBF_4) with molten aluminium alloy. The formation of reinforcement at the interface is mainly due to the kinetics and thermodynamics of the reaction between two salts and liquid aluminium. The TiB_2 formation in molten aluminium is illustrated in reactions (1) and (2).

$$(22/3)Al + 2KBF_4 + K_2TiF_6 \longrightarrow (1/3)K_3AlF_6 + 3KAlF_4 + AlB_2 + Al_3Ti \quad (1)$$

$$Al_3Ti + AlB_2 \longrightarrow TiB_2 + 4Al \quad (2)$$

The development of TiB_2 particulate reinforcement in the molten aluminium is depicted in reaction (2). And from reaction (1) it can be observed that unbalanced intermetallic components such as AlB_2 and Al_3Ti are formed due to lower reclamation of boron when KBF_4 is added in the stoichiometric proportion. To improve the reclamation of boron, potassium tetrafluroborate was added 20% more than the amount of stoichiometric ratio to attain TiB_2 and evade the development of intermetallic phases [19].

The requisite amounts of two salts needed were weighed to the desired weight fraction of TiB_2. To expel the engrossed moisture present, two fluxes were separately dried in a hot air oven at 150°C for 60 mins. The salts of suitable quantity were wrapped in aluminium foils that are to be added to the liquid aluminium alloy. In a vertical muffle furnace, the required amount of aluminium alloy was heated in a pre-heated crucible to a predetermined temperature of 860°C. Once the melt reached to 860°C the salts were added and stirred at a speed of 180rpm by a zirconia coated graphite stirrer for uniform mixing of salts and molten alloy mixture. To ensure uniform distribution and complete reaction of salts the whole mixture is held at 860°C for 60mins. To produce defect free composites the mixture was stirred for first and last 15 mins in a holding time of 60 mins. According to the above Equation (2), TiB_2 particulate formation was confirmed in the molten aluminium alloy by exothermically reaction of two salts (K_2TiF_6 and KBF_4). After the removal of slag, the superheated melt was poured into a plate-shaped cast mild steel mold of 100mm × 100mm × 10mm size. The samples for microstructure, corrosion, hardness and tensile tests were cut by using wire EDM machines.

2.3 Optical Microscopy and FESEM with EDS Analysis

The behavior of most metal alloys and composites can be determined by orientation, size of the grain, twins, shape and size, and distribution of secondary phases in the matrix alloy [20]. Various materials discontinuities, such as inclusions and stringers can also be detected microscopically. Those imperfections could assist initiation of failure sites in the materials, owing to this property of the materials and engineering reliability are to be adjudged through characterization of their shape, size and distribution [21]. Optical microscopy was done at Agro Met Lab, Coimbatore, India by using Dewinter trinocular metallurgical microscope, with specifications of magnification 50× to 1000×, objective lens magnification of 5× to 100× consuming a power of 12V, 50W Halogen lamp with polarizer prism. The polished composite samples were etched with 0.5% HF etchant and Optical micrographs were captured by a digital camera attached to the microscope. Field Emission Scanning Electron Microscope equipped with energy dispersive spectroscopy (EDS) was carried out by using SIGMA HV – Carl Zeiss with Bruker Quantax 200 – Z10 EDS Detector at CIT, Coimbatore, India to observe the microstructure, fracture morphology and elemental analysis of the cast samples.

2.4 XRD Analysis

X-ray diffraction is the scattering of x-ray photons by atoms in a periodic lattice. The scattered monochromatic x-rays that are in phase give constructive interference. This analysis was carried out by using X-Ray Diffraction with small angle scattering and polycrystalline equipment (XRD- Bruker AXS D8 Advance, Coimbatore, India) with a specimen size of 2cm × 1cm × 1cm.

2.5 Hardness Testing

Vickers micro hardness tests were performed by using micro hardness tester (Agro Met Lab, Coimbatore, India, Model: (FIE) Fuel Instrument and Engineering.) with a sample size of 2.5cm × 1.5cm × 1cm were cut as per ASTM standard E384-16 from a casted plate of AA7010-TiB_2 in-situ composite. Micro hardness tests were carried out with an indentation load of 300g for a holding time of 30sec. The test was conceded at three different locations on each specimen to obtain average hardness value and avoid possible effect of the indenter resting on the hard reinforcement particles.

2.6 Tensile Testing

The tensile tests with sample size of 9.2cm × 1cm × 1cm were conducted on a universal testing machine (Agro Met Lab, Coimbatore, India Model: PC-2000, Fuel Instrument and Engineering (P) Ltd) according to ASTM standard E370-14 with crosshead speed of 0.3 mm/min.

2.7 Corrosion testing method

Exfoliation corrosion is often observed in 2xxx (Al-Cu-Mg) and 7xxx (Al-Zn-Cu-Mg) series high strength alloys. This type of corrosion is characterized by lamellar surface attack of alloys containing a highly directional grain structure. The primary risk of exfoliation corrosion lies in the possible loss of actual cross section [22]. Exfoliation corrosion is usually intergranular in nature, owing to the galvanic relation between the adjacent matrix and grain boundary precipitates. The common exfoliation corrosion tests in laboratory that have been reported are immersion test method, salt spray method, electrochemical corrosion test and mechanical test. The first two methods usually involve in the interaction between alloys and acidic solution to determine the susceptibility of a certain alloy. The resulting surface is often compared to the environmental exposure data [23–25]. The specimens for testing the exfoliation corrosion (EXCO) were subjected to duration of 48 hours under artificial mimic environments of industrial or coastal areas. It depicts that the sample exposed to these types of environments resembles an equivalence period of 6 to 9 years. The prepared artificial environment is being formulated with test solution containing adequate quantity of reagent water mixed with chemicals that are highly corrosive. The corrosion rate was determined by conducting EXCO test as per ASTM G34 standard [26, 27]. Chemicals with specimens inside them were placed in an air tight non-reactive container (plastic) for 48 hours test duration. Specimens of size 2cmx1cmx1cm were cut as per the ASTM G34 standard and placed in a container fitted with an air tight cover to impede the evaporation of chemicals. Initial weights of the samples were noted after the specimens were cleaned with kerosene. 3M scotch pressure sensitive tape was used as a masking for the surfaces not to be exposed to the solution. A test solution was prepared which containing 50 g of potassium nitrate (KNO_3), 6.3 mL of nitric acid (HNO_3) and, 234 g of sodium chloride (NaCl), which were mixed together for 1Litre dilute solution for an approximate pH of 0.4. The specimens were immersed in an adequate quantity of solution for providing a ratio of volume to metal surface area with an approximation of 10 to 30 mL/cm^2 respectively at 28°C for time duration of 48 hours. To avoid the loss of material corroded from the metal surface the specimen surface were set to upward direction [28]. Corrosion rate (mm/year) was determined by considering the materials loss based on mass. After performing the procedure, using 50 vol.% nitric acid, specimens were washed, dried, and weighed.

3 Results and Discussions

3.1 X-ray diffraction (XRD) analysis of AA7010-TiB_2 Composites

XRD analysis was carried out on metallographically polished composite specimens. Figure 1 shows the XRD patterns attained for the cast in-situ composites and these confirm the presence of TiB_2 reinforcement within the matrix alloy. It is evident that in-situ formed TiB_2 particles and matrix aluminium alloy were clearly visible from the diffraction peaks. The peaks of TiB_2 reinforcement increase with the increase of TiB_2 content while the peaks of AA7010 decrease.

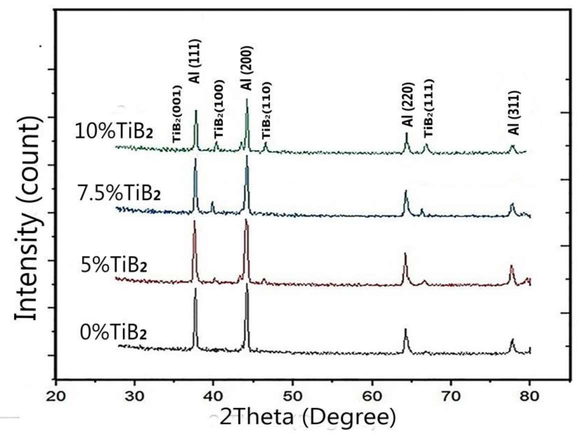

Figure 1: XRD Patterns of AA7010-TiB_2 in-situ composites

3.2 Microstructure Characterization

Figure 2 shows the optical images of as-cast AA7010-TiB_2 composite for different weight percentages of TiB_2 reinforcement. From the figures it is observed that single TiB_2 particles and TiB_2 clusters are homogeneously distributed with increase of reinforcement content with matrix alloy. Formation of dendritic structure is found in matrix alloy whereas, rosette-like irregular dendritic grain structure is observed in the developed composite. The homogenous distribution of TiB_2 is increased with increase of reinforcement concentration. Aluminium grain solidifies around the TiB_2 particulates which are behaving like nucleation center that provides resistance to the grain growth [29].

Figure 3 shows the FESEM images and EDS patterns of the as-cast sample composites produced with various wt% of TiB_2 in AA7010. FESEM images clearly show that the mechanical interactions between TiB_2 and AA7010 particles have been achieved. It can be understood that due to in-situ stir casting route with optimized process parameters, the development of TiB_2 clusters are avoided in the AA7010-TiB_2 composite. But indeed small salt inclusion can be observed in the FESEM images which are avoided by proper removal of slag. Increase of TiB_2 wt% provide sufficient wettability and bonding with the alloy. It is also observed that the TiB_2 particles are uniformly distributed in the liquid aluminium with very low agglomeration, which is due to the stirring of molten metal before and after 15 min during the holding time of 60min respectively. From EDS spectrums for all the as-cast composites elemental peaks of aluminum, titanium and boron and the chemi-

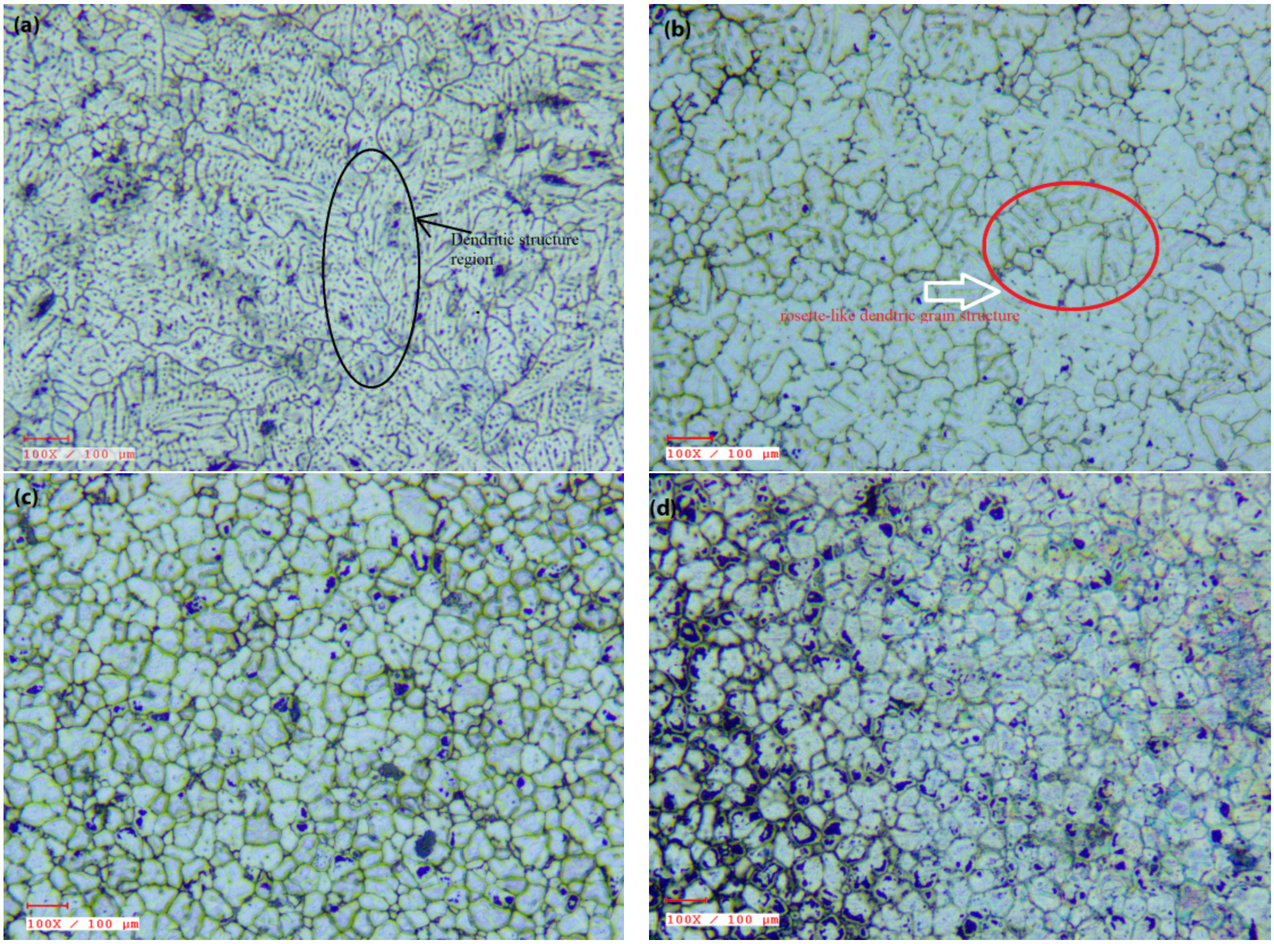

Figure 2: Optical images of as-cast AA7010/TiB_2 composite (a) 0% TiB_2, (b) 5% TiB_2, (c) 7.5% TiB_2 and (d) 10% TiB_2

cal composition identified with high intensity peak were zinc, magnesium, silicon, and ferrous which are alloying elements of AA7010. The extra elements like sodium, rhenium and tantalum were identified at very low peaks. It can be understood that from the elemental peaks and wt.% composition of aluminium, titanium and boron confirms the formation of TiB_2 at the interface [30].

3.3 Mechanical Properties

The average hardness values of AA7010 with different reinforcements of 0%, 5%, 7.5%, and 10% TiB_2 composites are 80 (SD=1.89), 100.5 (SD=6.33), 100.2 (SD=4.46) and 110.9 (SD=9.84) respectively. It is evident that as the weight% of reinforcement increases, the composite hardness also increasing owing to the occurrence of titanium diboride which acts as an advance strengthening phase in aluminum alloy matrix. The effect of strengthening for developed composites was increased due to the presence of TiB_2 which is very hard. Increase in hardness with a net value of 25-35% was reported in Figure 4 for different weight% of TiB_2. Crack growth is resisted due to the interaction between the reinforced TiB_2 particles and the dislocations leading to the improvement of hardness for the composite when compared with base alloy [31]. It is also observed that the hardness of 5% TiB_2 and 7.5% TiB_2 is nearly equal and decrease in the hardness value can be seen in 7.5% TiB_2 which may be due to poor particulate diffusion in aluminum because of limited stir time. Hardness of in-situ composite is also improved due to grain refining action of reinforcement with AA7010 alloy during solidification process.

The effect of addition of reinforcement with matrix alloy on Ultimate Tensile Strength (UTS) and Yield Strength (YS) (with error bars of 5%) is depicted in Figure 5 and 6 respectively. Addition of reinforcement with AA7010 develops maximum increase in UTS and YS of 260% and 240% for 10% TiB_2 respectively when compared with base alloy. It is also clear that maximum increase of UTS and YS is found to be with 7.5% and 10% TiB_2. It found that during

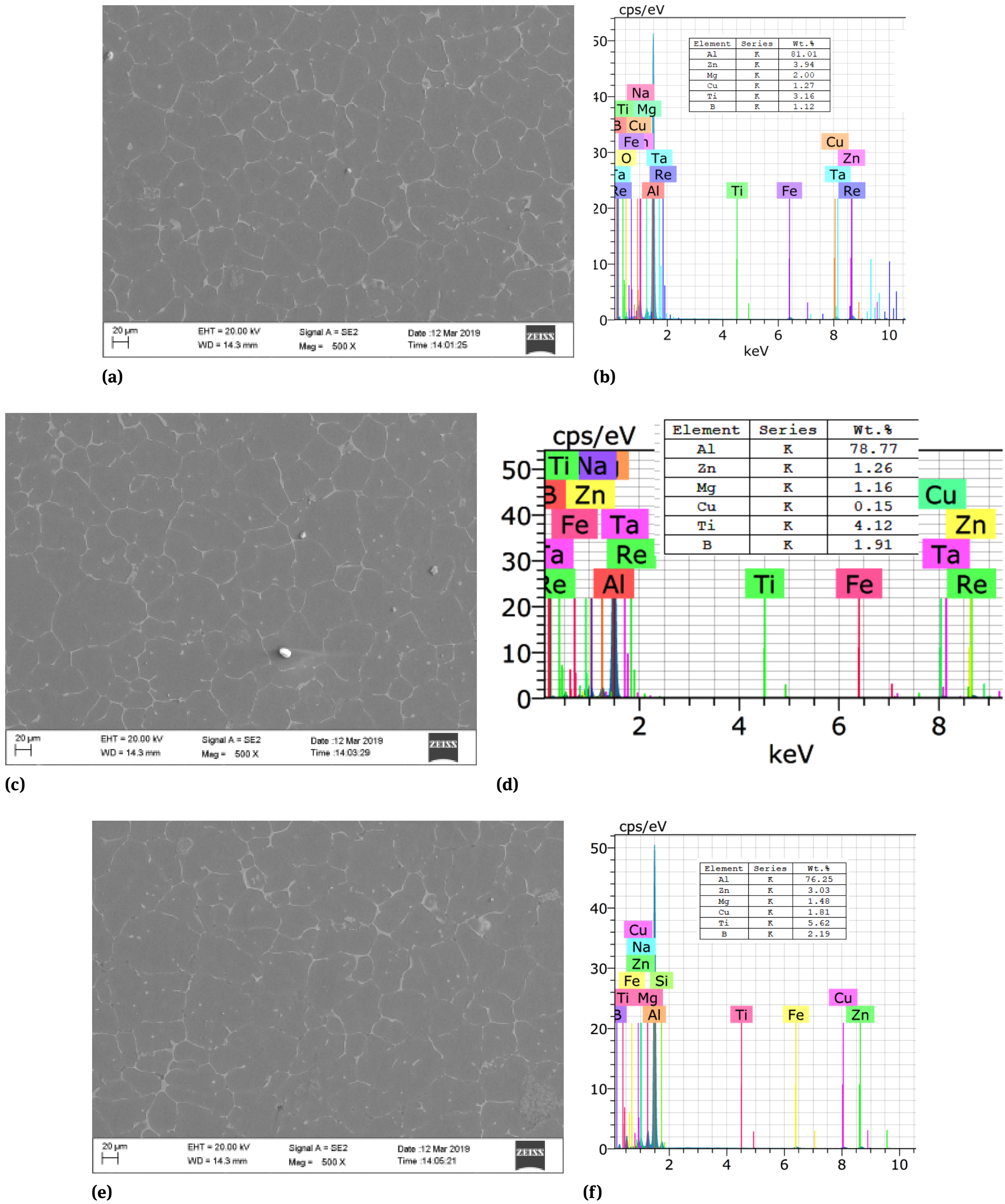

Figure 3: FESEM and EDS of AA7010-TiB_2 composites (a) & (b) 5% TiB_2, (c) & (d) 7.5% TiB_2 and (e) & (f) 10% TiB_2

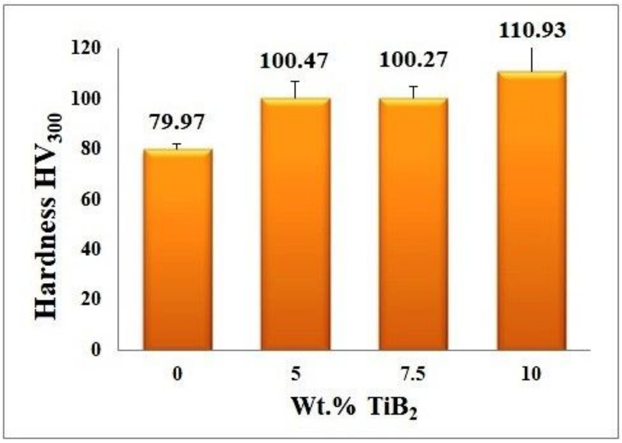

Figure 4: Effect of hardness for different wt.% of TiB_2

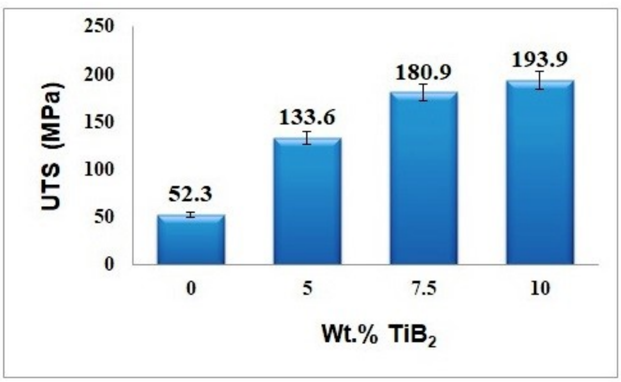

Figure 5: Ultimate Tensile Strength for AA7010 before and after addition of TiB_2 Reinforcement

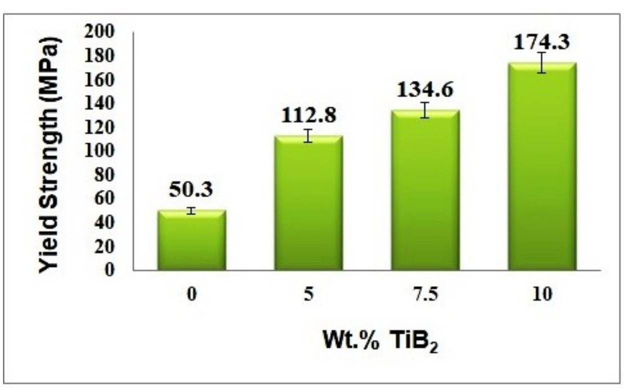

Figure 6: Effect of Yield Strength for various wt% of TiB_2

tensile loading the interaction between strong TiB_2 particulates and dislocations impedes the cracks propagation leading to increase of tensile properties. According to well known Hall-Patch relationship, grain refined in-situ TiB_2 particulates increase the area to resist the tensile loading and improves the strength of the composite. Owing to the existence of hard particulate reinforcement with a significant interaction between the dispersed hard particles and dislocations leads to homogeneously distributed TiB_2 particles which invoke Orowan strengthening mechanism [32]. This effect of particle strengthening in the matrix alloy is found to be improved with increase in the wt.% of reinforcement, where existence of hard TiB_2 particulates impedes the motion of dislocation by acting as a barrier in the composite under plastic deformation. Effect of elongation (with error bars of 5%) behavior of AA7010 reinforced with various wt.% of TiB_2 is as shown in Figure 7. In the current investigation composite elongation percentage improves by about 50% with 7.5% TiB_2, and 10% TiB_2 which is due to the refinement in grain that may hinders the propagation and crack growth in the developed composite. It is been observed that as the wt.% of increases percentage elongation increases for 7.5%, and 10% TiB_2, whereas % elongation decreases for 5% TiB_2 owing to the debonding of TiB_2 particles bands which may causes voids in the ductile matrix and easy propagation of crack leads to early failure [33].

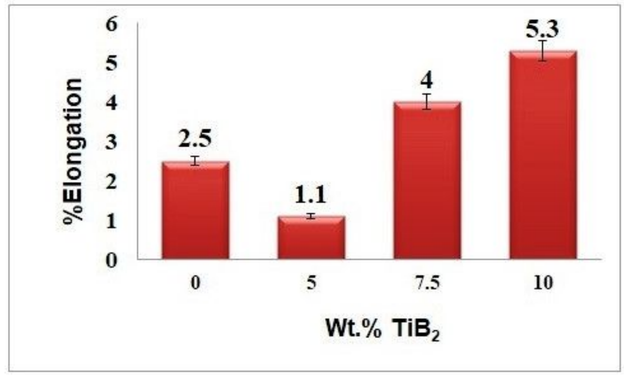

Figure 7: Elongation Behavior of AA7010/TiB_2 composites

3.4 Corrosion behavior of AA7010-TiB_2 composites

Corrosion behavior of Aluminium Metal Matrix Composite is mainly rely on various reasons and one of a reason on which the characteristics of cast or wrought depend is the processing methods used, type of matrix alloy, shape, size and type of reinforcement. The effect of corrosion is also happening due to the fabrication methods used for processing of MMC owing to the development of intermetallic phases between the reinforcement and base alloy. The strength or weakness of a composite is mainly depending on the interfacial bonding among the base alloy and the reinforcement. It is understood that interfacial bonding is the most significant parameter in the study of cor-

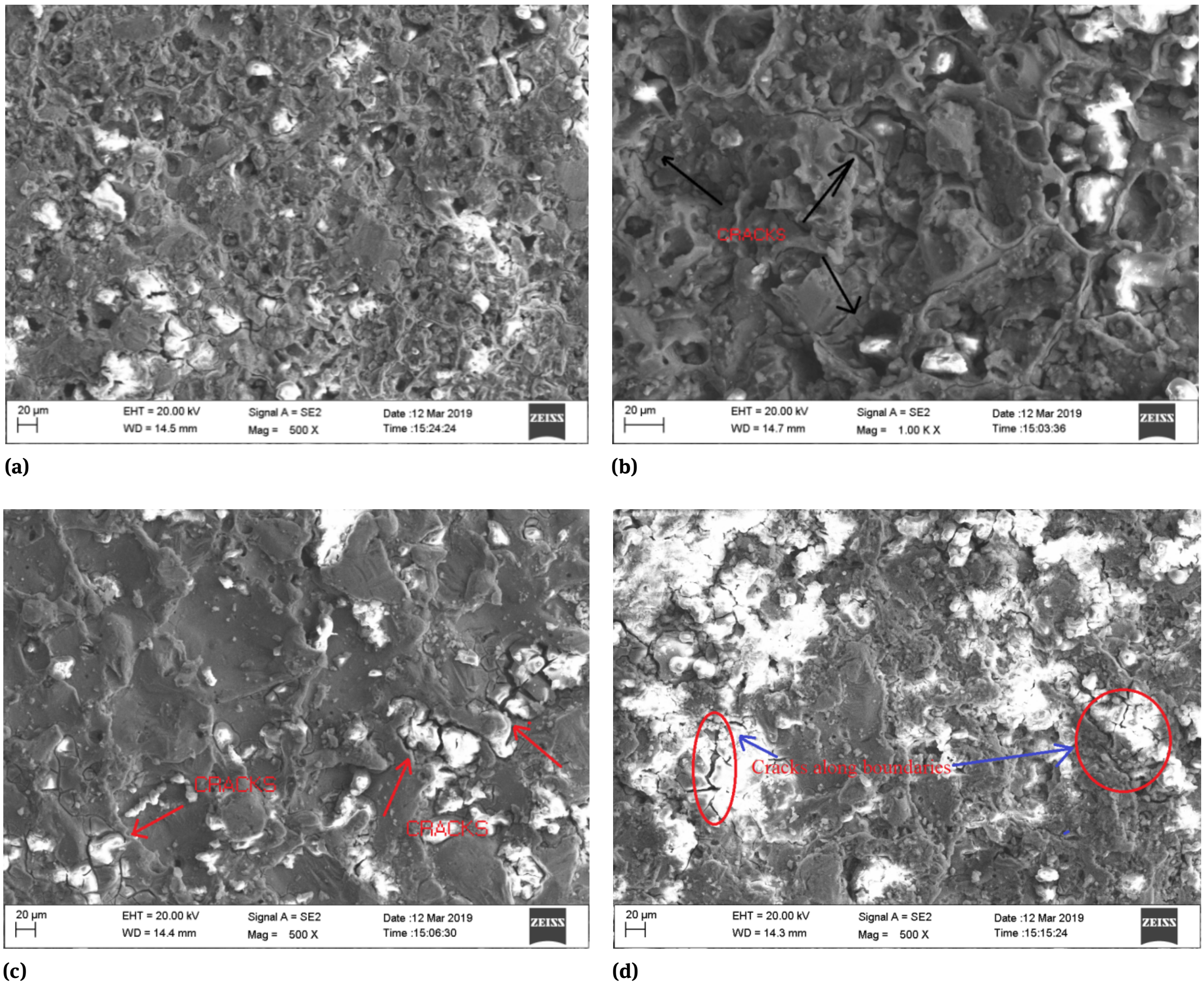

Figure 8: FESEM Analysis of corroded samples AA7010 - TiB_2 for (a) 0% TiB_2, (b) 5% TiB_2, (c) 7.5% TiB_2 and (d) 10% TiB_2

rosion, the improved corrosion resistance of the AA7010/ TiB_2 composite in the present work owes to a strong interfacial bond between the matrix alloy and reinforcement. Therefore, TiB_2 with increase in weight percentage leads to improvement in corrosion resistance of the composite [34]. The FESEM surface morphologies of the corroded samples for various wt.% TiB_2 (0%, 5%, 7.5%, and 10%) are shown in Figure 8. It can be perceived that exfoliation begins from pitting corrosion through intergranular corrosion to general corrosion at the end along the grain boundaries. Corrosion cracks are observed around the grain boundaries, which are regularly acting as a propagation path of exfoliation corrosion thereby a significant loss of metal with greater penetration, can be observed on the surface regions. Visual inspection on surface morphologies cannot determine the penetration depth of corrosion. Indeed the corrosion rate of the composite material can be calculated by using the following formula, on the basis of weight loss method for different wt% of TiB_2 [35]. The Table 2 shows corrosion rate behavior of cast aluminium metal matrix composites with various wt%. TiB_2 and it has been observed that while the wt% of TiB_2 increases, corrosion rate decreases. As we know that corrosion resistance of the ma-

Table 2: Corrosion rate of the Aluminium metal matrix composites

S.No.	wt.% of TiB_2	Corrosion rate mm/year
1.	0%	0.042
2.	5%	0.013
3.	7.5%	0.011
4.	10%	0.008

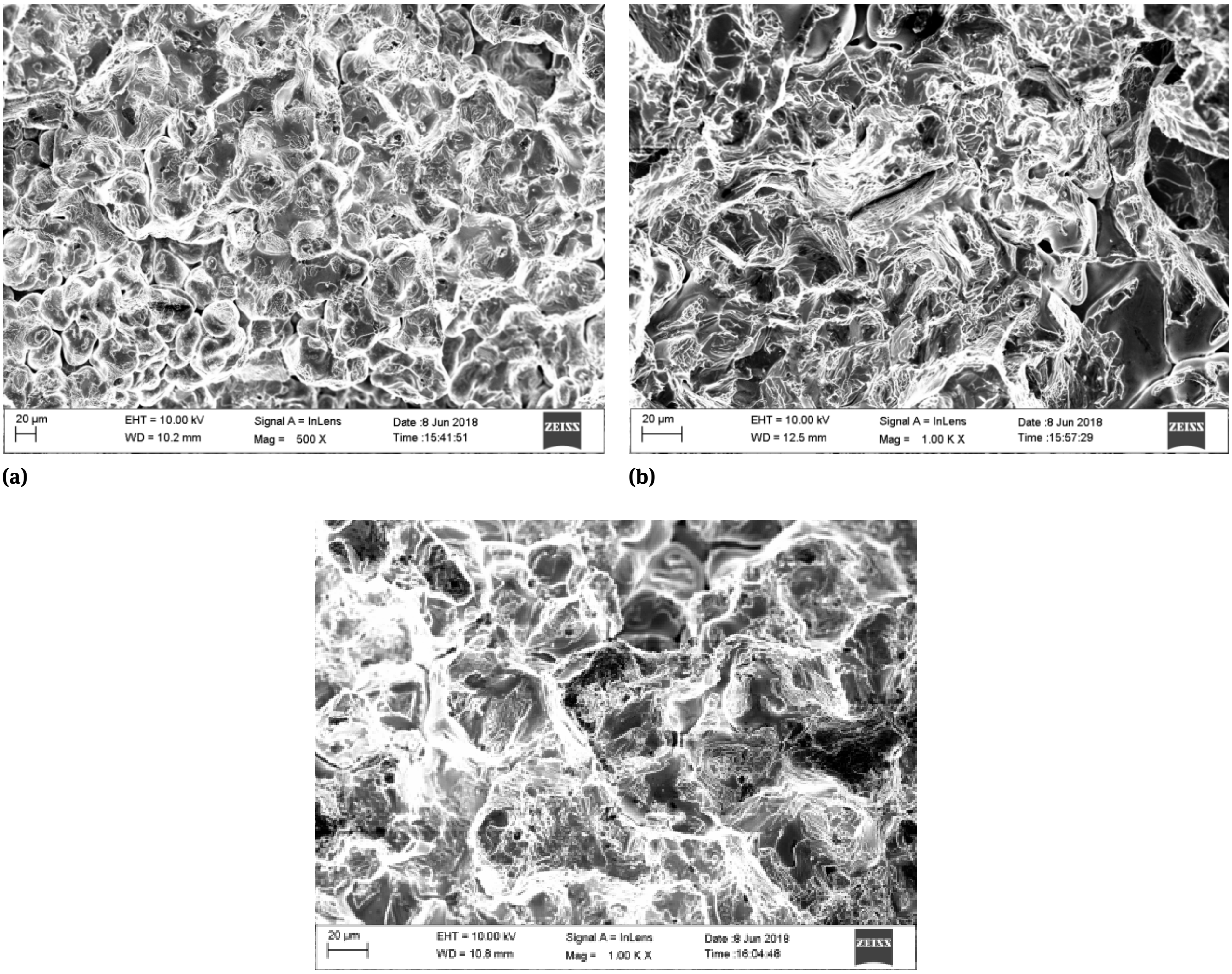

(a) **(b)** **(c)**

Figure 9: FESEM fractographs of TiB_2/AA7010 composites (a) 5% TiB_2, (b) 7.5% TiB_2 and (c) 10% TiB_2

terial is better with the reduction of corrosion rate.

$$Corrosion\ rate\ mm/year = \frac{87.6 \times weight\ loss}{\rho \times A \times T}$$

ρ = Specimen density in gm/cm^3
A = Area of specimen in cm^2
T = Exposure time in 24 hours.

3.5 Fractography

The AMMCs produced by the in-situ stir casting technique were tensile tested and the fracture morphologies for different %wt. TiB_2 are as shown in Figure 9. The morphologies indicate equiaxed dimples in large quantities which are surrounded by tiny dimples that control the fracture surface. The fracture of the composite still follows the ductile nature of the aluminum alloy regardless of the incorporated stiff reinforcement. Indeed the TiB_2 particles are acting as effective barriers in coalescence and growth of voids. From the above results it confirms that the strong interfacial bonding and wetting can be attained using the in-situ stirring technique between the matrix and reinforcement [36].

4 Conclusions

AA7010/TiB_2 AMMC was successfully produced by the in-situ reaction of inorganic salts such as K_2TiF_6 and KBF_4 to liquid aluminum. The in-situ reaction between the halide salts and aluminium alloy resulted in the growth of TiB_2 as reinforcement. In the present study, effects of the different wt.% reinforcement on grain structure refinement, mechanical properties and rate of exfoliation corrosion in the newly developed AA7010- TiB_2 composites were discussed.

- The in-situ stir casting method is suitable for fabricating ceramic reinforced metal matrix composite with homogenous particle distribution and less porosity, which is visualized from the optical micrographs. FESEM and EDS analysis reveals the uniform distribution of reinforcement with low agglomeration for the stirring of molten metal at first and last 15 min in total holding time of about 60min and for a stirrer speed of 800 rpm respectively. EDS spectrum confirms the formation of TiB_2 reinforcement with the matrix alloy.
- From laboratory immersion test, rate of exfoliation corrosion is been identified by weight loss method, where the results revealed that corrosion rate of the in-situ composites are reduced about 80.95% with addition of TiB_2 reinforcement to the matrix alloy.
- Fractography images conforms that the newly developed AA7010-TiB_2 composite failure still follows the ductile nature irrespective of the incorporated stiff reinforcement. Whereas the reinforcement avoids the coalescence and hinders the void growth.
- From the above studies it can be suggested that AA7010 with 10% TiB_2 shows better results with respect to mechanical and corrosion properties when compared with 5% TiB_2, 7.5% TiB_2 and matrix alloy

References

[1] Hull D, Clyne TW. An Introduction to Composite Materials. New York: Cambridge University Press; 1996. https://doi.org/10.1017/CBO9781139170130.

[2] Krishan K. Chawla, Composite Materials Science and Engineering. 3rd ed. New York: Springer; 2011.

[3] Dipti Kanta Das, Purna Chandra Mishra, Saranjit Singh and Ratish Kumar Thakur Properties of ceramic-reinforced aluminium matrix composites - a review International Journal of Mechanical and Materials Engineering 2014 1:12 doi:https://doi.org/10.1186/s40712-014-0012-9.

[4] Hashim J, Looney L, Hashmi MS. Metal matrix composites: production by the stir casting method. J Mater Process Technol. 1999;92:1–7.

[5] Kumar M, Gupta RK, Anand PA. Review on Fabrication and Characteristics of Metal Matrix Composites Fabricated By Stir Casting IOP Conf. Series. Mater Sci Eng. 2018;377:012125.

[6] Pramod SL, Srinivasa R. Bakshi, and B.S. Murty Aluminum-Based cast in-situ Composites: A Review. J Mater Eng Perform. 2015;24(6):2185–207.

[7] Lakshmi S, Lu L, Gupta M. In situ preparation of TiB2 reinforced Al based composites. J Mater Process Technol. 1998;73(1-3):160–6.

[8] Lu L, Lai MO, Chen FL. In situ preparation of TiB2 reinforced Al base composite. Adv Compos Mater. 2012;6(4):299–308.

[9] Kumar N. Gaurav Gautam, Rakesh Kumar Gautam, Anita Mohan and Sunil Mohan Synthesis and Characterization of TiB_2 Reinforced Aluminium Matrix Composites: A Review J. Inst. Eng. India Ser. D Metallurgical & Materials and Mining Engineering; 2015. https://doi.org/10.1007/s40033-015-0091-7.

[10] Michael Rajan HB, Ramabalan S, Dinaharan I, Vijay SJ. S.J. Vijay Synthesis and characterization of in-situ formed titanium diboride particulate reinforced AA7075 aluminum alloy cast composites. Mater Des. 2013;44:438–45.

[11] Jebeen Moses J, Dinaharan I. S. Joseph Sekhar Prediction of influence of process parameters on tensile strength of AA6061/TiC aluminum matrix composites produced using stir casting. Trans Nonferrous Met Soc China. 2015;26(6):1498–511.

[12] Akshay Mohan Pujar and Chetan Kulkarni Study of Mechanical Properties and Microstructure of Aluminium Alloy Reinforced with TiB2, by in-situ Technique Materials, Energy and Environment Engineering proceedings of ICACE 2015 DOI https://doi.org/10.1007/978-981-10-2675-1_2.

[13] Chen F. ZongningChen, FengMao, TongminWang, and Zhiqiang Cao TiB_2 reinforced aluminum based insitu composites fabricated by stir casting. Mater Sci Eng A. 2015;625:357–68.

[14] S.G.Pantelakis and A.T.Kermanidis Corrosion Control in the Aerospace Industry Woodhead Publishing Series in Metals and Surface Engineering 2009 67-108.

[15] E.A. Starke, Jr and J.T. Staley Fundamentals of Aluminium Metallurgy Production, Processing and Applications Woodhead Publishing Series in Metals and Surface Engineering 2011 747-783.

[16] Choudhury A, Gopakumar A, Athul KP. D R Adinath and Mrudula Prashanth Experimental analysis of Exfoliation rate on Aluminum alloy Al7010 IOP Conf. Series. Mater Sci Eng. 2017;225:012037.

[17] Bobby-Kannan M, Raja VS, Raman R, Mukhopadhyay AK. Influence of Multistep Aging on the Stress Corrosion Cracking Behavior of Aluminum Alloy 7010. Corros Sci. 2003;59(10):881–9.

[18] Ajay Krishnan M, Raja VS. Development of high strength AA 7010 aluminum alloy resistant to environmentally assisted cracking. Corros Sci. 2016;109:94–100.

[19] S.Suresh and N.Shenbga Vinayaga Moorthi Aluminium- Titanium Diboride (Al-TiB_2) Metal Matrix Composites Challenges and Opportunities Procedia Engineering 2012 38 89-97.

[20] Whan R E, Materials Characterization, Volume 9, ASM International, USA, 1986.

[21] Voort G F V. Metallography, and Microstructures. ASM Handbook. Volume 9. USA: ASM International; 2004. https://doi.org/10.31399/asm.hb.v09.9781627081771.

[22] Standard Test Method for Exfoliation Corrosion Susceptibility in 2xxx and 7xxx Series Aluminum Alloys (EXCO Test)", in Annual Book of ASTM Standards, American Society for Testing and Materials, 1990 114-119.

[23] Robinson MJ, Jackson NC. Exfoliation corrosion of high strength Al–Cu–Mg alloys: effect of grain structure. Br Corros J. 1999;34(1):45–9.

[24] Lee S, Lifka BW (Agarwala VS, Ugiansky GM, editors). Modification of the EXCO Test Method for Exfoliation Corrosion Susceptibility in 7XXX, 2XXX and Aluminum Lithium Alloys. American Society for Testing and Materials; 1992. https://doi.org/10.1520/STP19577S.

[25] Conor PC, James AD, Collier RN. Evaluation of Exfoliation Corrosion Damage to 7075-T6 Aluminum Alloy Aircraft Structural

Components Materials and Structures Group. Defense Technology Agency; 2004.

[26] Zhao X. Exfoliation Corrosion Kinetics of High Strength Aluminum Alloys, Ph.D. thesis, The Ohio State University, 2006.

[27] International A. ASTM G34-01(2013) Standard Test Method for Exfoliation Corrosion Susceptibility in 2XXX and 7XXX Series Aluminum Alloys (EXCO Test). West Conshohocken (PA): ASTM International; 2013.

[28] International A. Standard Guide for Conducting Exfoliation Corrosion Tests in Aluminum Alloys. West Conshohocken (PA): ASTM International; 2015.

[29] Suresh S, Moorthi NS. Process Development in Stir Casting and Investigation on Microstructures and Wear Behavior of TiB2 on Al6061 MMC. Procedia Eng. 2013;64:1183–90.

[30] Suresh S, Shenbaga Vinayaga Moorthi N, Vettivel SC, Selvakumar N. Mechanical behavior and wear prediction of stir cast Al–TiB2 composites using response surface methodology. Mater Des. 2014;59:383–96.

[31] Rengasamy NV, Rajkumar M, Senthil Kumaran S. Mining environment applications on Al 4032 – Zrb 2 and Tib 2 in-situ composites. J Alloys Compd. 2016;658:757–73.

[32] Chen Z, Kang H, Zhao Y, Zheng Y, Wang T. The role of TiB2 in strengthening TiB2 reinforced aluminium casting composites IOP Conf. Series. Mater Sci Eng. 2016;117:012039.

[33] Jeshurun Lijay K, David Raja Selvam J, Dinaharan I. S.J.Vijay Microstructure and mechanical properties characterization of AA6061/TiC aluminum matrix composites synthesized by in-situ reaction of silicon carbide and potassium fluotitanate. Trans Nonferrous Met Soc China. 2016;26(7):1791–800.

[34] Zakaria HM. Microstructural and corrosion behavior of Al/SiC metal matrix composites. Ain Shams Eng J. 2014;5(3):831–8.

[35] Lu X, Han X, Du Z, Wang G, Lu L, Lei J, et al. Tietao Zhou Effect of microstructure on exfoliation corrosion resistance in an Al-Zn-Mg alloy Elsevier. Mater Charact. 2018;135:167–74.

[36] Pazhouhanfar Y, Eghbali B. Microstructural characterization and mechanical properties of TiB_2 reinforced Al6061 matrix composites produced using stir casting process. Mater. Sci. Eng. A. 2018;710:172–80.